JOURNAL OF GEOPHYSICAL RESEARCH, VOL. 102, NO. A12, PAGES 27,109-27,119, DECEMBER 1, 1997

On the internal radial structure of field line resonances

Ian R. Mann [1]

Astronomy Unit, Department of Mathematical Sciences, Queen Mary and Westfield College
London, England

Abstract. We examine the radial scales developed inside field line resonances (FLRs) when they are driven by both broad and narrow frequency bandwidth fast mode sources. The finest FLR radial scales are always limited by ionospheric dissipation, being determined primarily by the height-integrated Pedersen conductivity Σ_P. We estimate likely FLR radial scale sizes in both dayside and nightside ionospheric conditions, and confirm the accuracy of these estimates using the wave Doppler shifts observed on inbound/outbound passes of Active Magnetospheric Particle Tracer Explorers CCE [*Anderson et al.*, 1989]. Dayside broadband FLR events can have radial scale lengths significantly shorter than their overall widths, suggesting they may possess several radial amplitude nodes and antinodes. Further, we examine the Kelvin-Helmholtz (KH) stability of FLRs due to their azimuthal velocity shear. We estimate a FLR toroidal velocity threshold, for particular Σ_P, beyond which the KH growth rate is sufficiently large to disrupt the FLR. For typical magnetospheric conditions, FLRs are not likely to be disrupted by driving secondary KH vortices. For large-amplitude FLRs in regions of high Σ_P, however, it may be possible for FLRs to be disrupted by the KH instability and to develop into large-scale KH vortices. We further speculate on the possible link between auroral zone FLR internal radial scales and the observed optical widths of discrete auroral arcs.

1. Introduction

Since the initial ground-based magnetometer observations of *Samson et al.* [1971], a large amount of theory has been developed to understand the spatial and polarization structure of field line resonances (FLRs). Notably, the seminal papers by *Southwood* [1974] and *Chen and Hasegawa* [1974] were the first to derive the modal structure of pulsations including fast and Alfvén wave coupling. Early works considered monochromatic Kelvin-Helmholtz (KH) magnetopause surface waves as the likely FLR energy source, with later developments suggesting the possibility of fast cavity eigenmodes being created between an internal wave turning point and an outer boundary (usually the magnetopause) [*Kivelson et al.*, 1984; *Kivelson and Southwood*, 1985, 1986; *Allan et al.*, 1985, 1986]. The cavity eigenmode picture was subsequently modified to include the opening of the magnetosphere downtail to form a waveguide [e.g., *Samson et al.*, 1992a]. These theoretical treatments usually involve the calculation of the structure of wave normal modes, the theory having developed into a considerable success with the observed variations of ULF wave period and polarization with latitude being accurately reproduced.

Ground-based observations often show FLRs to be monochromatic over a range of latitudes, with the latitude of maximum amplitude (the "resonant" field line) increasing with increasing wave period. This is clearly in good accord with the modal theories of *Southwood* [1974] and *Chen and Hasegawa* [1974]. Satellite observations however, show that pulsations often exhibit L shell dependent frequencies, believed to result from the oscillations of field lines at their local Alfvén frequency, and frequently display a nearly uniform amplitude over a large range of L shells. L dependent oscillations of this type, observed, for example, by Active Magnetospheric Particle Tracer Explorers (AMPTE) CCE, are believed to be excited by broadband sources of some kind; *Hasegawa et al.* [1983] pointed out the theoretical possibility of pulsations being driven by a broadband disturbance.

Whilst the normal modes of a system are useful tools for examining the mathematical details of wave morphology, any real system's behavior will result from a summation or integration over the governing eigenmodes [see, e.g., *Wright and Allan*, 1996a, and references therein]. In an inhomogeneous ideal plasma, the eigenmodes are singular at the Alfvén resonance. In a realistic time dependent situation, energy can be seen to be accumulated at the "resonance," with the wave fields remaining well behaved in both space and time [*Barston*, 1964; *Goedbloed*, 1983; *Cally*, 1991; *Mann*

[1] Now at Department of Physics, University of Alberta, Edmonton, Canada.

Paper number 97JA02385.
0148-0227/97/97JA-02385$09.00

et al., 1995; *Cally and Maddison*, 1997]. In this paper we suggest that both the broadband L dependent oscillations over a range of latitudes, and the more monochromatic classical FLR responses, can naturally be represented by a summation over the eigenmodes of the magnetospheric system. Each eigenmode in the inhomogeneous magnetosphere represents a coupled fast and Alfvénic disturbance having a single eigenfrequency. Any time-dependent response of the magnetosphere can then be synthesized using these eigenmodes (the Barston modes). The broadband scenario could result from the excitation of a wide range of eigenmodes by a large-frequency bandwidth energy source, whilst the classical narrowband FLR response usually observed on the ground can be understood as resulting from only a few eigenmodes being dominantly driven in the magnetosphere, perhaps being excited by KH vortices on the flank magnetopause, or by magnetospheric ringing in response to a sudden impulse. It is possible that only the narrowband FLR events are observed with resonant characteristics by ground-based magnetometers, whilst the broadband events have period and amplitude characteristics which are smeared by the magnetometers spatial integration [*Poulter and Allan*, 1985]. This smearing might result in the observation of an apparently fixed frequency over a range of latitudes; their frequencies decreasing with increasing latitude (this appears to be the case in the ground magnetometer signatures of the L dependent oscillations reported by *Lin et al.* [1992]). This could resolve the contradiction of why monochromatic FLRs are observed from the ground, but L dependent frequency oscillations are often seen in situ in the magnetosphere.

In this paper we examine the internal radial structure of FLRs by considering the fields which we expect to result when waves are driven by different sources. In each case, we can understand the pulsation physics by considering the fields as a summation over the eigenmodes. We use the observations of differing inbound and outbound pulsation frequencies in the AMPTE CCE data set reported by *Anderson et al.* [1989] to infer the internal scale lengths of dayside broadband pulsations and compare it to theoretical estimates based on height-integrated ionospheric Pedersen conductivities (Σ_P). Further, we consider the likely differences in the scale sizes of dayside versus nightside waves and speculate on the likelihood of the shearing equatorial FLR velocity fields to be subject to the KH instability. We qualitatively estimate the conditions necessary for the KH instability to be sufficiently strong to disrupt a FLR of particular amplitude oscillating on field lines with footpoints in conditions of varying Σ_P. Finally, we discuss the possible link between FLRs and discrete auroral arcs.

2. Internal FLR Radial Structure

In a recent study, *Mann et al.* [1995] used a time-dependent model to show how the overall radial width of a FLR can be understood in terms of the bandwidth of the driving fast wave as it deposits energy around the resonant field line. In the absence of dissipation, the overall radial width of the resonance should narrow in time ($\propto t^{-1}$) until it reaches a scale which is determined by the driver's frequency bandwidth. The wider the bandwidth of the driver, the broader the resulting overall spatial width of the toroidal fields at the resonance. The final full width at half maximum (FWHM) ΔX, as found, for example, in the velocity perturbations, is

$$\Delta X \sim \Delta\omega \left(\frac{d\omega_A}{dx}\right)^{-1}, \quad (1)$$

where $\Delta\omega$ is the bandwidth of the driver's velocity field (FWHM), and $d\omega_A/dx$ is the local Alfvén frequency gradient.

For example, if the magnetosphere acts as a high-quality factor (Q) resonant cavity, then the cavity/-waveguide response to a sudden impulse, for example, will have a narrow bandwidth and can be described using a summation over only a few Barston modes. The cavity disturbance should drive a narrow FLR resonant response centered on the resonant field line; the spatial width being determined by the bandwidth which the cavity mode develops due to its amplitude decay, including cavity losses and the deposition of energy at the "resonance" [*Mann et al.*, 1995]. Widths $\sim$ 0.4 R_E are predicted for typical theoretical cavity mode "decay" rates, in good agreement with the observed widths of impulsive cavity mode driven FLRs [e.g., *Yeoman et al.*, 1997]. Similarly, monochromatic KH surface waves on the magnetopause should drive similar narrow resonances, whilst low Q cavity/waveguide modes, broadband KH magnetopause surface waves, or simply broadband inwardly propagating fast waves should drive much wider resonances, requiring a large number of Barston modes to be used to synthesize the broadband waves.

Once the energy has been deposited at the resonance, the resulting toroidal FLR fields tend to oscillate at the local natural Alfvén frequency. Over time, the field lines drift out of phase with each other and generate increasingly fine internal structure, having phase mixing length scales given by [*Mann et al.*, 1995]

$$L_{ph}(t) = 2\pi \left(\frac{d\omega_A}{dx} t\right)^{-1}. \quad (2)$$

In an ideal plasma, and on field lines with no ionospheric losses, the eigenmodes of an inhomogeneous plasma are singular at the resonance; the ξ_x (poloidal) fields governed by a logarithmic ($\ln(x - x_r)$) singularity, and the ξ_y (toroidal) fields are governed by a $1/(x - x_r)$ singularity. These singular eigenmodes (the Barston modes) can be used as a basis set of functions with which to describe the real time-dependent evolution of coupled MHD waves [*Barston*, 1964; *Cally*, 1991; *Mann et al.*, 1995; *Cally and Maddison*, 1997]. It is the singularities in the eigenmodes which allow ideal phase mixing to continue without limit, producing toroidal length scales which continuously narrow in time; the eigenmode singularities also being responsible for the asymptotically toroidal wave state produced by time-dependent FLR wave evolution [*Radoski*, 1974].

In the Earth's magnetosphere, dissipation in the ionosphere removes the singularities in the ideal eigenmodes and limits their finest scales [*Wright and Allan*, 1996b]. FLR eigenmodes varying as $\exp i(k_y y - \omega t)$ and standing along the background field with a wavenumber k_z in a box model magnetosphere [e.g., *Southwood*, 1974] can be described in terms of universal functions $\mathcal{F}$ and $\mathcal{G}$ where [*Wright and Allan*, 1996b]

$$\xi_x = \xi_{x0} e^{i\phi} \mathcal{G}(X); \quad \mathcal{G}(X) = \ln(X - i) \quad (3)$$

$$\xi_y = -\xi_{xo} \frac{e^{i\phi}}{k_y \delta_B} \mathcal{F}(X); \quad \mathcal{F}(X) = \frac{-i}{(X-i)}. \quad (4)$$

Here $X = (x - x_r)/\delta_B$, and

$$\delta_B = -2\frac{k_{zi}}{k_{zr}} \left(\frac{\omega^2}{d\omega_A^2/dx}\right)_{x_r} = \left(l\mu_0 \Sigma_P \left. \frac{d\omega_A}{dx} \right|_{x_r} \right)^{-1} \quad (5)$$

(field lines have length $2l$, Σ_P is the height-integrated Pedersen conductivity, and k_z is as given by *Wright and Allan* [1996b], having a real part k_{zr} which represents the wave's standing nature and an imaginary part k_{zi} describing the ionospheric damping). The familiar logarithmic ξ_x and $1/x$ ξ_y eigenmode behavior is clearly apparent. The toroidal fields of these eigenmodes (represented by ξ_y) have a spatial scale determined by the universal function $\mathcal{F}$. The physical spatial x scale L_m of $\mathcal{F}$ is given approximately by $L_m \sim 4\delta_B$ and is $\propto \Sigma_P^{-1}$. Hence higher ionospheric conductivities generate finer spatial scales. Similarly, the v_y velocity shear ($v_y = d\xi_y/dt$) in $\mathcal{F}$ occurs over a length scale of $\sim 2\delta_B \sim L_m/2$ [see *Wright and Allan*, 1996b, Figures 6 and 8]. Again this shear length scale is narrower for higher Σ_P.

In the case of continually driven pulsations, using a phase mixing argument, *Mann et al.* [1995] had earlier shown how FLR radial widths would decrease in time ($\propto t^{-1}$) and eventually develop a limited radial scale size. Adopting a dynamical argument in terms of a superposition of Alfvén waves, *Mann et al.* [1995] argued that FLR fields would be continually driven with relatively large amplitude and spatial scale. The waves excited at a given time would phase mix more and more the longer they lived; however, they would also decay in amplitude and become more insignificant. Consequently, the ionosphere limits the finest spatial scales which the phase mixing can generate and produces an asymptotic ionospherically limited radial scale length L_I.

Assuming that the wave amplitudes become insignificant after two ionospheric decay times (i.e., after a time $t = 2\tau_I$; $\tau_I = 1/\gamma$ and γ represents the ionospheric damping) gives

$$L_I \sim \pi \left(\frac{d\omega_A}{dx}\tau_I\right)^{-1}. \quad (6)$$

Physically, L_I represents the length scale developed by phase mixing in a time $2\tau_I$. Note that *Mann et al.* [1995] used $t = \tau_I$ in their definition of L_I; however, after this time waves have only decayed to $\sim 34\%$ of their original amplitude. Using $t = 2\tau_I$ allows waves to decay down to $\sim 10\%$ (which can be considered insignificant); the dominant scale of the evolving waves being likely to be $\gtrsim L_{ph}(t = 2\tau_I) = L_I$. The fact that ionospheric dissipation removes the singularities in the eigenmodes means that in a dynamically evolving time-dependent situation we expect the finest scale sizes developed by the system to be limited to the scalelengths of the eigenmodes (this is obvious since they can be used as a basis to construct physical (x, t) solutions). Indeed, using the time $t = 2\tau_I$ to define L_I makes the two expressions for ΔX_ξ in (32) and (33) of *Mann et al.* [1995] (representing L_I and L_m) consistent to within 10% (W. Allan, personal communication, 1997).

Since fast and Alfvén waves are subject to very different ionospheric boundary conditions, fast waves typically being much better reflected and less strongly damped [*Kivelson and Southwood*, 1988], the bandwidth of the fast mode driver (be it a cavity/waveguide disturbance, a KH magnetopause surface wave or even a broadband inwardly propagating fast wave disturbance) should be relatively unaffected by Σ_P. Consequently, in all cases the finest internal radial structure field line resonances can develop will be determined by the relative sizes of ΔX and L_I. In the next section we examine the likely internal structure of broadband toroidal FLR oscillations (specifically those observed by AMPTE CCE and reported by *Anderson et al.* [1989]) and other more narrowband FLRs.

3. FLR Radial Scalelengths

3.1. Broadband Toroidal FLR Observations

Anderson et al. [1989] completed a statistical study of strongly toroidal dayside pulsation events displaying the characteristic of L dependent frequencies over a wide range of L shells, between 0500-0900 magnetic local time (MLT) and $L = 4-9$ (note that for distances beyond $\sim 5R_E$ 0500 MLT field lines map to the dayside ionosphere). This probably represents a situation where the waves are being continually driven by some broadband source. Assuming that the waves oscillated at the local Alfvén frequency $\omega_A(\mathbf{r})$, *Anderson et al.* [1989] assumed a wave variation $b \sim b_0 \exp i\psi$, where

$$\psi = \omega_A(\mathbf{r})(t - t_0(\mathbf{r})) - \mathbf{k}(\mathbf{r}).\mathbf{r} \quad (7)$$

for $t > t_0$, and $\psi = 0$ for $t < t_0$. Here t_0 is the onset time of the disturbance, and $t - t_0$ is the time the field lines have been ringing for. *Anderson et al.* [1989] showed that the apparent frequency observed by CCE (ω') would be shifted relative to the actual local Alfvén frequency $\omega_A(r_0)$ due to the phase mixing of the ringing field lines, so that

$$\omega' = \frac{d\psi}{dt} = \omega_A(r_0) + (t - t_0)(\mathbf{V_{CCE}}.\nabla)\omega_A(\mathbf{r}) \quad (8)$$

where r_0 is the position of the observation, and $\mathbf{V_{CCE}}$ is the velocity of AMPTE CCE at r_0, that is, $\omega' = \omega_A(r_0) + \delta\omega$, where $\delta\omega$ is the frequency change resulting from the phase mixing of the waves. They found that the frequency shift $\delta\omega$ was opposite for inbound and outbound trajectories, as would be expected on the basis of the phase mixing theory, with a typical magnitude $\delta\omega/\omega_A \sim 0.1$. Figure 6 of *Anderson et al.* [1989] clearly illustrates this behavior. It shows the apparent frequencies ω as a function of L observed by AMPTE CCE on inbound and outbound passes, with the inbound and outbound $\omega(L)$ curves being displaced relative to the average over the total ensemble of events from all the CCE passes.

On the basis of these frequency shifts, *Anderson et al.* [1989] calculated an average ringing time of $\tau_{\rm data} = t - t_0 \sim 800 - 1200$ s. Since each event is observed at an unknown time during the wave's evolution, an average of the observed ringing time should give a statistical estimate for the ionospheric decay time. We have argued that the radial scales generated by phase mixing will be limited to L_I, so we can identify $\tau_{\rm data}$ with $2\tau_I$, and hence calculate the scale lengths of the waves $L_{\rm data}$ inferred from the CCE observations. Using the modeling of *Allan and Knox*, [1979a,b] in a dipole magnetic field, we can compare model $2\tau_I$ with $\tau_{\rm data}$ to test the validity of the theory. The model of *Allan and Knox,* [1979a,b] has a density which varies $\propto L^{-q}$ in the equatorial plane and $\propto r^{-6}$ along the field lines and generates an Alfvén frequency variation [see also *Allan and Knox*, 1980]

$$\omega_A(L) = C\frac{L^{-a}}{\sqrt{(L-1)}}. \quad (9)$$

Here L is the McIlwain parameter, C is a constant, $a = (7 - q)/2$, and we take $q = 4$ for waves outside the plasmapause. The Alfvén frequency gradients are hence given by

$$\frac{d\omega_A(L)}{dL} = -\omega\left\{\frac{2L - 1.5}{L(L-1)}\right\}. \quad (10)$$

We consider the particular event presented by *Anderson et al.* [1989] in their plate 2, where L dependent oscillations were seen between $L \approx 4 - 7$ with frequencies $\sim 25 - 10$ mHz. Using the observed frequency of 10 mHz at $L = 7$, knowing at $L = 7$ CCE crosses L shells at a rate of $V_{\rm CCE} \sim 2.6 \times 10^{-4}$ R_E s^{-1}, and assuming $\delta\omega/\omega = 0.1$, we find a ringing time for this event of $t - t_0 = 1290$ s. Setting this time equal to $2\tau_I$ produces an estimated damping decrement of $\gamma/\omega \sim 0.025$ (using $\gamma = 1/645$ s^{-1}) and a radial length scale $L_{\rm data} \sim 0.26$ R_E. The overall width of the disturbance was observed to be $\Delta X \gtrsim 3$ R_E, which suggests that these pulsations had several radial oscillations inside the overall radial envelope of the wave (since $L_{\rm data} < \Delta X$). This is schematically illustrated in Figure 1a.

We can confirm the hypothesis that the radial scales inside FLRs are governed by L_I by comparing the observed ringing times with the theoretical ionospheric damping times calculated by *Allan and Knox*, [1979a,b]. Using the observed period of 100 s (10 mHz waves) at $L = 7$ and considering the waves to be second harmonic, we find ionospheric damping decrements γ/ω and asymptotic phase mixing lengths L_I as a function of Σ_P as given in Table 1. (Note that the damping decrements are not strongly dependent on the harmonic number but are strongly dependent on wave period.) Higher Σ_P generates smaller length scales L_I, as expected. Considering a typical dayside conductivity of

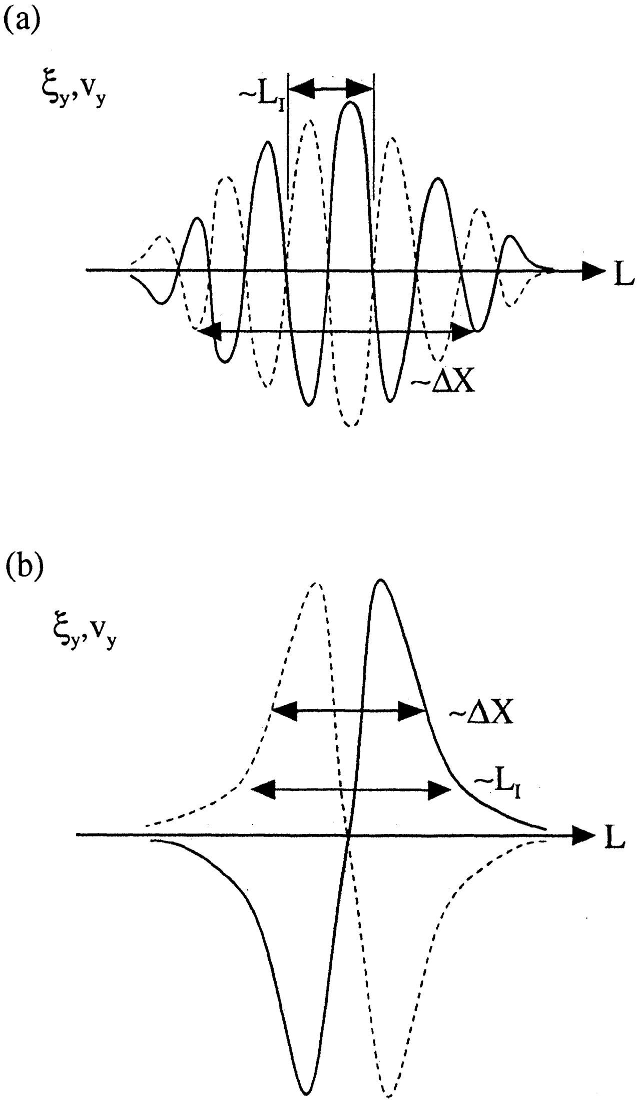

Figure 1. Schematic diagram of FLR toroidal fields. Solid lines show the FLR fields; dashed lines depict the fields half a period later. (a) Broadband FLR: Continually driven by a broad frequency bandwidth source, having $\Delta X > L_I$. (b) Narrowband FLR: Displaying the classical $1/x$ FLR phase and amplitude signature, having $\Delta X \sim L_I$.

Table 1. Pulsation Radial Widths for Second Harmonic Waves at $L = 7$ (100 s Period)

Σ_P, S	Ionospheric γ/ω	L_I, R_E
1	0.183	1.93
4	0.041	0.43
6	0.028	0.29
8	0.021	0.22
10	0.017	0.18
20	0.008	0.08
30	0.005	0.05

Table 2. Pulsation Radial Widths for Fundamental Mode Waves at $L = 8$ (360 s Period)

Σ_P, S	Ionospheric γ/ω	L_I, R_E
1	0.698	8.46
4	0.129	1.56
6	0.085	1.03
8	0.064	0.77
10	0.051	0.62
20	0.025	0.31
30	0.017	0.21

$\sim 6-8$ S gives a theoretical $\gamma/\omega \sim 0.021-0.028$ (representing $L_I \sim 0.22-0.29\ R_E$), which is in excellent agreement with apparent damping decrement (γ/ω) and the scale length L_{data} from the dayside AMPTE CCE observations presented above. Clearly, the ringing times estimated from the Doppler shifts in the data are of the same order as theoretical dayside ionospheric decay times. This gives good experimental verification to the suggestion of *Mann et al.* [1995] that the internal radial scale lengths for these continually driven oscillations can be estimated using (6).

3.2. Narrow Bandwidth FLR Observations

In this section we consider the radial structure of FLRs driven by more monochromatic fast mode disturbances. *Mitchell et al.* [1990] observed a FLR with an overall width $\Delta X \lesssim 0.5\ R_E$ with ISEE 1 and ISEE 2, which was possibly driven by a KH magnetopause surface wave disturbance, and which subsequently displayed oscillations at the local Alfvén frequency after the cessation of power input from the KH wave. Consequently, the wave would have an overall width $\sim \Delta X$; the toroidal fields subsequently phase mixing and decaying due to ionospheric dissipation. We can compare this value of ΔX to the lengths L_I developed inside fundamental mode FLRs. We choose waves with 360 s period at $L = 8$ to facilitate a comparison of the observations of *Samson et al.* [1996] of a FLR coexisting at the location of discrete auroral arcs, which we consider further in section 5.

Again using the results of *Allan and Knox*, [1979a,b], we find damping decrements γ/ω and lengths L_I as a function of Σ_P as given in Table 2. Interestingly, this suggests that longer-period (lower harmonic) waves only have time to generate relatively large phase mixing scales during their ionospheric lifetime. Based on Table 2, we expect long-period (fundamental mode) FLRs on the dayside to have $L_I \sim \Delta X$. Waves with the classical FLR signature of an amplitude enhancement and a π phase change over a narrow range of L shells (found, for example, by *Southwood* [1974], and in subsequent work using more realistic geometries [e.g., *Wright and Thompson*, 1994]) should correspond to these cases where $L_I \sim \Delta X$. This scenario is schematically illustrated in Figure 1b. Based on Table 2, we suggest that for fundamental mode FLRs on the dayside L_I is typically $\sim \Delta X$. At locations where Σ_P is enhanced (e.g., in the auroral zone), however, L_I will be significantly reduced and can become $< \Delta X$.

Interestingly, since $L_I \propto \omega^{-1}$ (combining (6) with (10)), higher harmonic waves are more likely to have internal structure inside the width ΔX because they can phase mix to finer scales within their ionospheric lifetimes. The observations of *Anderson et al.* [1989] were of harmonic frequency ($\sim$ 10-25 mHz) waves which are likely to have finer internal scales than fundamental mode waves and hence which are likely to have larger Doppler shifts when observed in situ by satellites. In all cases, we anticipate that the finest scales ever developed inside a FLR can be estimated on the basis of the scale lengths developed due to ionospheric dissipation. In the next section we use L_I as an estimate for the equatorial radial length scales inside FLRs and hence analyze their likely Kelvin-Helmholtz stability for conditions of various Σ_P.

4. Kelvin-Helmholtz Stability of FLR Toroidal Fields

The possibility that magnetospheric FLRs might excite the KH instability because of their azimuthal velocity shear has recently been suggested [*Rankin et al.*, 1993a; *Samson et al.*, 1996]. In the context of solar coronal heating, the action of the KH instability inside FLRs has previously been considered by *Hollweg and Yang* [1988], the KH instability being suggested as a possible mechanism for enhancing the plasma heating rate. Similarly, *Browning and Priest* [1984] considered the KH stability of phase-mixed shear Alfvén waves, also proposing that the instability could enhance the heating inside phase-mixed wave fields. Note, however, that in the solar application, the action of viscosity or resistivity in the body of the plasma forms the dominant dissipation mechanism, and it is this which limits the scale lengths of the eigenmodes rather than the resistivity of the (ionospheric) boundaries.

The KH instability clearly favors large amplitude shears (which for fundamental mode magnetospheric FLR occurs in the equatorial plane), with the most unstable KH wave being described by azimuthal wavenumbers $k_{y\text{KH}}$ given by

$$k_{y\text{KH}} \sim 0.6/\Delta \tag{11}$$

where Δ is the thickness of the region of velocity shear [*Walker*, 1981]. Earlier in this paper we estimated the finest radial scales which might be developed during FLR evolution; ionospheric dissipation playing a crucial role in determining their finest radial scales and hence the length over which the FLR velocity field's shear acts. Previous workers using models with perfectly conducting ionospheric boundaries have imposed FLR scales as small as $\sim 0.1\ R_E$ [e.g., *Rankin et al.*, 1993b]. We believe that the effect of the lower bound on the radial length scales can be critical in determining whether magnetospheric FLR fields are stable to the KH instability, and we examine this below.

Assuming that the waves are incompressible for simplicity, KH surface waves have a zero real eigenfrequency and have a growth rate governed by their imaginary wave frequency $\omega_{i\mathrm{KH}}$, given by

$$\omega_{i\mathrm{KH}}^2 \approx k_{y\mathrm{KH}}^2 v_{yR}^2, \tag{12}$$

where v_{yR} is the FLR azimuthal velocity amplitude (i.e., the FLR in this model experiences a shear of $2v_{yR}$), see appendix.

Since the FLR velocities v_{yR} oscillate from having maximum to zero shear on a timescale of $T_R/4$, where T_R is the FLR standing Alfvén wave period, and numerical studies by *Rankin et al.* [1993a] show how the KH instability is quenched and does not disrupt the FLR for waves with growth times longer than this, we can define a critical e-fold KH growth rate $\omega_{\mathrm{crit}} = 2\omega_{rR}/\pi$, where ω_{rR} is the real FLR frequency. Using (11) for the fastest growing KH modes azimuthal (y) wavenumber, we can define a critical radial scale length Δ_{crit} given by

$$\Delta_{\mathrm{crit}} = 0.3\pi\frac{v_{yR}}{\omega_{rR}} = 0.15 v_{yR} T_R. \tag{13}$$

The FLR velocity shear length scale (Δ_{vs}) must be greater than Δ_{crit} in order for the FLR not to be disrupted by the KH instability. This criterion estimates how narrow FLR velocity shear layers should be in order for velocity fields of magnitude v_{yR} to drive KH vortices which destroy the FLR.

Using the results of *Allan and Knox*, [1979a,b] in a dipole geometry, we can use (6) to define the FLR velocity shear length, being given by $\Delta_{vs} \sim L_I/2$. For any particular wave, this will relate Σ_P and v_{yR} to create the criterion for KH instability from (13) (i.e., $\Delta_{vs} < \Delta_{\mathrm{crit}}$ for instability). Now

$$\frac{L_I}{2} \sim \frac{\pi L(L-1)R_E}{2(2L-1.5)}\left|\frac{\gamma}{\omega}\right| \tag{14}$$

$$\frac{\gamma}{\omega} = \frac{2}{m\pi}\ln\left(\frac{\Sigma_P - \zeta_I}{\Sigma_P + \zeta_I}\right) \tag{15}$$

where $\zeta_I = (2\mu_0 A_0 Z_0)^{-1}$, and $A_0 = 8R_E L Z_0/mT_R$ is the equatorial Alfvén velocity which is chosen to model the required wave frequency ω_{rR}. $Z_0 = (1-1/L)^{\frac{1}{2}}$ and the numbers $m = 2, 4, 6\ldots$ represent the field-aligned harmonics of half-wavelength modes with ionospheric velocity nodes. Consequently, the instability criterion is given by

$$\frac{L(L-1)R_E}{(2L-1.5)m}\ln\left|\left(\frac{\Sigma_P - \zeta_I}{\Sigma_P + \zeta_I}\right)\right| < 0.15 v_{yR} T_R. \tag{16}$$

Expanding out the logarithm for $\zeta_I/\Sigma_P \ll 1$, then $\ln[(\Sigma_P - \zeta_I)/(\Sigma_P + \zeta_I)] \approx -2\zeta_I/\Sigma_P$, and considering fundamental mode waves ($m = 2$) the instability criterion becomes

$$\Sigma_P v_{yR} > \frac{[L(L-1)]}{1.2\mu_0 L(2L-1.5)Z_0^2} \tag{17}$$

(Note that the instability criterion is only weakly dependent on L, and in this limit is independent of ω_{rR}.) For example, at $L = 8$ the instability criterion is

$$\Sigma_P v_{yR} > 3.66 \times 10^5, \tag{18}$$

(Σ_P in siemens, and v_{yR} in m s^{-1}). Considering $\Sigma_P = 6$ S would require $v_{yR} > 61$ km s^{-1}, implying that a large total velocity shear in excess of ~ 120 km s^{-1} is required at the resonance for dayside FLRs to become disrupted by the KH instability. FLRs whose footpoints lie in regions of lower Σ_P would require even greater velocity shears for the KH instability growth rates to be large enough to destroy the FLR.

In Figure 2 we show the critical v_{yR} as a function of Σ_P. FLRs with equatorial v_{yR} above these curves, for given Σ_P, will be disrupted by KH waves. It should be stressed that the velocity criterion probably represents a lower limit because we have assumed incompressibility and that the FLR velocity fields shear over an infinitesimal layer when estimating $\omega_{i\mathrm{KH}}$. A more realistic treatment to include the effect of the shear layer's width on $\omega_{i\mathrm{KH}}$ would require numerical computation [e.g., *Rankin et al.*, 1993a]. However, our point here is to emphasize that the effect of Σ_P limiting the FLR

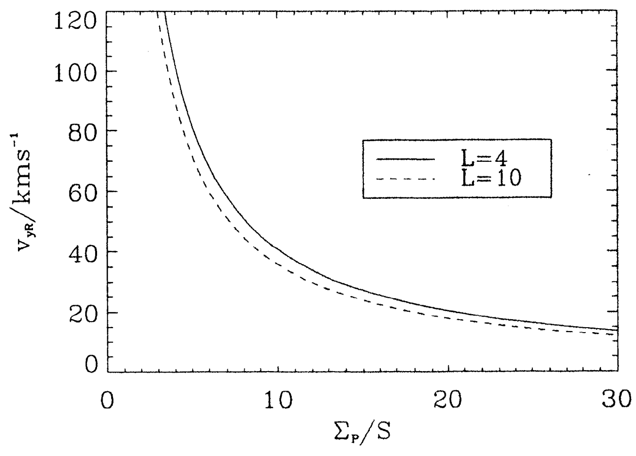

Figure 2. The critical azimuthal velocity (v_{yR}) required for fundamental mode FLRs to be disrupted by driving KH waves plotted as a function of Σ_P (calculated using (17)).

scales may be at least as important as the magnitude of the FLRs azimuthal velocity shear. We discuss the implications for the KH disruption criterion in the following section.

5. Discussion

From the analysis presented in the previous section, we can estimate the likely KH stability of FLR velocity fields of particular amplitude in regions of differing ionospheric Pedersen conductivity Σ_P. Estimating the magnitudes of FLR velocities from satellite data, however, is difficult. Fundamental FLRs have equatorial antinodes in ξ, **v** and **E**, and nodes in **b**. The majority of satellite FLR observations present wave trains observed in **b**, which cannot be used to estimate **v** since the ratio **b**/**v** for these standing waves varies strongly along the field line, especially near the **b** field node at the equator.

Observations of **E** can be used to calculate **v** from the frozen field condition ($\mathbf{E} + \mathbf{v}_\wedge \mathbf{B_0} = 0$). Poloidal (rather than toroidal) Alfvén waves observed by *Singer et al.* [1982] showed $|E_y| \sim$ a few mV m^{-1}. A toroidal wave with a similar equatorial $|E_x| \sim 1$ mV m^{-1} at $L = 7$ would have $v_{yR} \sim 11$ km s^{-1}. Similar fundamental mode wave electric fields were measured using the GOES 2 satellite by *Junginger and Baumjohann* [1984], typical amplitudes being ~ 0.3 mV m^{-1}, representing typical velocities ~ 2.8 km s^{-1}. More GOES 2 observations presented by *Matthews* [1987] showed wave amplitudes between 0.5 and 9.0 mV m^{-1}, typically being $\sim 2 - 5$ mV m^{-1}, that is, velocities of $\sim 18 - 46$ km s^{-1}. For typical dayside Σ_P, these waves would probably not be disrupted by the KHI. The largest event (9.0 mV m^{-1}) observed by *Matthews* [1987], however, would have an equatorial velocity amplitude of ~ 80 km s^{-1}. This could easily be greater than the KH instability criterion for dayside conductivity.

Probably the best way to estimate the magnitude of equatorial FLR azimuthal velocities is to map the ionospheric wave electric fields observed by radar into the equatorial plane. Using the dipole model of *Walker* [1980], we estimate that at $L = 7$, $\left|\Sigma_P E_I / n_{\mathrm{eq}}^{0.5} E_{\mathrm{eq}}\right| \sim 7 \times 10^{-3}$, where E_I and E_{eq} are the magnitudes of the electric fields at the ionosphere and the equator respectively and n_{eq} is the equatorial electron number density [*Walker*, 1980, Figure 2b]. Considering the four FLR events observed with the Scandinavian Twin Auroral Radar Experiment (STARE) radar having electric field amplitudes of 12 (two observations) 16 and 44 mV m^{-1} reported by *Greenwald and Walker* [1980] [see also *Walker et al.*, 1979] produces equatorial azimuthal velocity amplitudes of ~ 20, ~ 26 and ~ 75 km s^{-1} (we have used $B_0 = 91$ nT at $L = 7$, $n_{\mathrm{eq}} = 3 \times 10^7 \mathrm{m}^{-3}$, $\Sigma_P = 6$ S and assumed the wave is a fundamental FLR so that $|v_{yR}| = |E/B_0|$ at the equator in a dipole field). All but the largest-amplitude event are again probably too small to cause the KHI growth rates to be sufficient to disrupt the FLR fields. The 44 mV m^{-1} event, however, represents a particularly large-amplitude FLR. The actual amplitude of the waves in this event may have been much larger than those apparently observed by STARE. This is because large electron drift velocities ($V_e \gtrsim 400$ m s^{-1}, representing $E \gtrsim 20$ mV m^{-1}) in the ionospheric E region sampled by STARE are limited by the action of the ionospheric two-stream instability [*Nielsen and Schlegel*, 1985]. The actual E field (and hence the velocity amplitude) for this event could be $\sim 1 - 3$ times greater than the apparent velocity recorded in the STARE data. Consequently, it is possible that this large-amplitude event was disrupted by the action of the KH instability. We should also note that in the model of *Walker* [1980], E_{eq} increases with Σ_P. If the electric fields seen by STARE are typical, this could also imply larger equatorial velocity shears for higher Σ_P conditions. Combined with the decrease in L_I with increased Σ_P, this could result in a significant enhancement of the KHI growth rates for FLRs situated in regions of enhanced ionospheric conductivity.

The only definite equatorial magnetospheric velocity observation known to the author comes from *Mitchell et al.* [1990]. They observed a very large amplitude FLR with $v_{yR} \gtrsim 100$ km s^{-1} in the dawn flank of the magnetosphere (dayside ionosphere). Since dayside Σ_P is typically $\sim$ 5-10 S [*Wallis and Budzinski*, 1981], this event could possibly have been converted into a vortex by the KHI. Indeed, as pointed out by *Rankin et al.* [1993a], *Mitchell et al.*'s wave event had comparable radial and azimuthal velocity components which is not inconsistent with the wave having developed a KH vortex. Similarly, using radar observations, *McDiarmid et al.* [1994] reported a large-amplitude FLR, believed to have been excited by an impulsively generated cavity/waveguide mode, with signatures in both the morning and afternoon flanks. The afternoon sector showed a classical FLR signature, whilst the morning sector displayed a traveling vortex signature, which could have resulted from the nonlinear development of the FLR fields via the KHI. For typical magnetospheric conditions, we predict that most FLRs are not disrupted by the KHI. This is reassuring since FLRs are observed very frequently in the magnetosphere. Probably, only the very largest amplitude FLRs, whose footpoints lie in ionospheric regions of high conductivity, are likely to decay into KH vortices.

In recent years there has been a resurgence of interest in the possible link between nightside auroral zone FLR and electron acceleration in discrete auroral arcs. A body of evidence is developing to suggest that FLR form an important aspect of auroral physics [*Samson et al.*, 1991, 1992b; *Xu et al.*, 1993; *Samson et al.*, 1996]. Some recent theoretical work has suggested mode conversion to electron inertial Alfvén waves may be responsible for the electron acceleration [see, e.g., *Streltsov and Lotko*, 1995, 1996, and references therein], although a causal link remains to be proven conclusively. *Samson et al.* [1996] provide some particularly convincing evidence for a link between FLRs and discrete auroral arcs, using radar, ground-based magnetometer, and optical observations. During their event, at a particular time, the discrete arc develops a vortex structure, which they suggest may be a signature of the FLR developing into a KH vortex in the equatorial plane, with the resultant vortex then propagating down to the ionosphere. Prior to the onset of the vortex, the discrete arc was observed to brighten. If the FLR fields are responsible for the acceleration of the arc's precipitating electrons, this could signify an amplitude enhancement of the FLR. Moreover, enhanced electron precipitation could also increase Σ_P at the FLR footpoints, possibly allowing the radial length scale of the FLR (and hence the length scale of its velocity shear) to narrow. The combination of these two effects could result in the FLR satisfying the KH disruption criteria, resulting in the observed auroral arc vortex.

Perhaps the most convincing evidence for links between FLR and discrete auroral arcs comes from the optical observations of the poleward motion of bands of discrete arcs. FLRs situated on field lines outside the plasmapause (where ω_A decreases with increasing L) are expected to show poleward phase propagation [*Greenwald and Walker*, 1980; *Wright and Allan*, 1996b]. The similarity between radar observations of poleward phase motion in FLRs, and the optical observations of poleward moving discrete arcs is remarkable (compare, e.g., Figure 2 of *Fenrich et al.* [1995] and Figure 3 of *Samson et al.* [1996]). Very recently, *Shiokawa et al.* [1996] have shown a Sun-aligned morning flank auroral arc event where small arc structures repeatedly appeared at the edge of a coexisting discrete arc and moved poleward in a quasi-periodic fashion, with a period of several minutes. Their arc structure mapped to an equatorial position well inside the magnetopause and occurred during a period of northwards interplanetary magnetic field (IMF). The authors had no explanation for the poleward motion of the arcs; pointing out that if an MHD disturbance propagating in from the flank magnetopause were responsible for the arc motions then they would have moved equatorward rather than poleward. If, however, the arcs coexisited at the location of an FLR, then the motion observed can be naturally explained by the physics of the poleward phase propagation of FLR fields. In many optical auroral arc observations, arc elements appear to show exactly the same poleward propagation behavior on the same timescales as FLR fields. This suggests a strong connection between discrete auroral arcs and FLRs, but the causal link whereby the electrons are accelerated directly in the FLR fields remains to be proven conclusively.

The optical observations of *Samson et al.* [1996] suggest an overall discrete auroral width (containing several arcs) of $\sim 50 - 60$ km in the ionosphere, each discrete arc being ~ 10 km wide. Mapping these to the equator to a distance of $\sim 8\ R_E$ produces scales of $\sim 0.7 - 0.8\ R_E$ and $\sim 0.13\ R_E$, respectively. These figures are in good agreement with the hypothesis that the overall width of the discrete arc structures is the same as ΔX (which can typically be $\gtrsim 0.5\ R_E$ for FLRs outside the plasmapause), and the hypothesis that the individual arc widths are given by $\sim L_I/2$. Assuming $\Sigma_P = 20$ S inside the arc structure would predict an arc width of $\sim 0.15\ R_E$ from Table 1, translating to ~ 11 km in the ionosphere, in excellent agreement with the observations. This suggests that it may be possible for nightside auroral zone Σ_P to be sufficient to allow FLRs in this region to have radial structure inside their overall spatial envelope (i.e., $L_I < \Delta X$), as was the case for the broadband dayside FLRs observed by *Anderson et al.* [1989] and discussed in section 3.

We have shown above that FLR physics can explain both the occurrence of multiple discrete arcs inside an overall arc structure (when $L_I < \Delta X$) and can account for the observed poleward arc phase motions. An important question which remains, however, is by which mechanism the FLR interacts with the discrete arcs. If FLRs fields are responsible for discrete arc electron acceleration via mode conversion to inertial Alfvén waves then this could explain the observations and provide a causal connection between FLRs and discrete arcs. However, we should be cautious about this interpretation. Current theories proposing FLRs as accelerators of precipitating discrete arc electrons via mode conversion to inertial Alfvén waves rely on the generation of very fine spatial scales of the order of the electron inertia length. As we have discussed in this paper, ionospheric dissipation prevents the creation of spatial scales finer than $\sim L_I$, and this will have a profound effect on whether FLR scales can become sufficiently small for the mode conversion to occur.

FLR simulations performed by *Wei et al.* [1994], which included electron inertial effects, showed the electron inertia was important once scales were $\lesssim 2\pi l_e$, where l_e is the electron inertia length given by $l_e = c/\omega_{pe} = \sqrt{m_e/\mu_0 n_e e^2}$. Using typical ionospheric and equatorial electron number densities of 10^{11} m^{-3} and 10^7 m^{-3} respectively, requires the FLRs to possess length scales $L_I \lesssim 2\pi l_e$, that is, $\lesssim 10$ km at the equator and $\lesssim 100$ m at the ionosphere. Even allowing for dipole field line convergence, these length scales are $\gtrsim 100$ times smaller than the L_I likely to be generated inside FLRs by phase mixing (both at the equator and at the ionosphere).

Consequently, some other additional mechanism is required if FLRs are to be responsible for discrete arc electron precipitation. For example, a significant additional electron density depletion in the auroral accelerator region ($\sim 2\ R_E$ above the ionosphere) might allow l_e to become sufficiently large for mode conversion to occur. For example, assuming $n_e = 0.5$ cm^{-3} [cf. *Borovsky*, 1993] at an altitude of 2 R_E above the ionosphere at $L = 7$, then $l_e = 7.5$ km, whilst an equatorial $L_I = 0.3\ R_E$ (representing $\Sigma_P = 20$ S) would map to ~ 150 km. In this case L_I in the accelerator region would be now only ~ 3.25 times larger than $2\pi l_e$. However, as discussed by *Borovsky* [1993], if the wave length scales are only a factor of 4 larger than $2\pi l_e$ then the wave dispersion and the resultant electron acceleration are reduced by orders of magnitude. Another possibility is the presence of unusually high Alfvén frequency gradients (called "isolated density boundary layers" by

Streltsov and Lotko [1995]). These might allow the local Alfvén frequency gradients to become large enough to reduce L_I sufficiently to induce the mode conversion ($L_I \propto (d\omega_A/dx)^{-1}$; see (6)). Observational evidence for the existence of these gradient enhancements is limited, although density enhancements were seen by *Hughes and Grard* [1984].

An alternative explanation is that the features of FLR structure and phase motion are apparent in the optical auroral observations because the FLR wave fields modulate the electron precipitation but are not themselves responsible for the actual electron acceleration via mode conversion to electron inertial Alfvén waves. The modulation of optical auroral light at the same frequency as coexisting giant ULF pulsations (Pgs) in the early morning MLT sector is well known [see, e.g., *Chisham et al.*, 1990, and references therein]. A variety of mechanisms have been proposed to explain the observed modulation [see, e.g., *Southwood and Hughes*, 1983; *Xu et al.*, 1993, and references therein], some of which might be operative in discrete arcs.

Another possibility is that the intense field-aligned currents (FACs) present inside FLRs induce plasma waves such as electrostatic ion-cyclotron waves via topside current instabilities [*Kindel and Kennel*, 1971]. These secondary plasma waves could provide the anomalous resistivity required to generate the field-aligned electric fields which accelerate the precipitating electrons [e.g., *Greenwald and Walker*, 1980]. If the auroral zone FLRs have internal structure of the form illustrated in Figure 1a, they would possess several upward and downward FAC current pairs, which could result in the production of several discrete arc structures. This would avoid the requirement for the arcs to have widths as small as electron inertial scale lengths. Certainly, the discrete arcs observed by *Samson et al.* [1996] appear to have widths greater than the likely electron inertial lengths, unless there is a sufficently low electron density somewhere along the field line. More detailed observations in the auroral accelerator region might allow these theories to be tested further.

6. Conclusions

In this paper we have analyzed the widths likely to be developed by FLRs, including the effects of ionospheric dissipation in limiting their radial scale lengths. We concluded that FLR morphology can be summarized as follows:

1. The overall width ΔX of a FLR is determined predominantly by the bandwidth of the driving fast mode wave source (i.e., $\Delta X \sim \Delta\omega(d\omega_A/dx)^{-1}$).
2. Once the fast mode energy has been deposited at the resonance, so that the fast mode forcing has been removed, the field lines oscillate at their local Alfvén eigenfrequencies generating fine scales $\sim L_{ph}(t) \propto t^{-1}$.
3. Phase mixing proceeds for a finite time, corresponding to the ionospheric lifetime of the waves, and generates ionospherically limited length scales L_I. These scales are as narrow as those developed due to ionospheric dissipation in the eigenmodes of the system.
4. For all FLRs, the finest scales, and hence the finest length scales over which the toroidal velocities shear, is determined by ionospheric dissipation.
5. The length scales which are phase mixed to in an ionospheric lifetime are shorter for higher-frequency waves. Waves with $L_I < \Delta X$ can have internal nodes and antinodes of wave velocity; this internal structure being more likely for harmonic rather than fundamental mode FLRs in regions of dayside Σ_P. In regions of strongly enhanced Σ_P, such as in the auroral zone, fundamental mode L_I can be $< \Delta X$ generating internal radial fine structure.
6. Even for very strongly enhanced active auroral ionospheric Pedersen conductivities (e.g., $\Sigma_P \sim 20$ S), L_I appears to be very much greater than the likely electron inertial length scales required if FLRs are to be responsible for the direct acceleration of discrete arc electrons via mode conversion to electron inertial Alfvén waves.
7. For the majority of FLRs, we estimate that the growth rates of KH vortices driven by FLR azimuthal velocity shear are too small for them to disrupt the FLR structure. Consequently, FLR radial structure can be expected to be similar to the schematic presented in Figure 1. It has recently been suggested, however, that the resulting small-amplitude KH waves might act as seeds for energetic particle-driven high-m Alfvén waves [*Allan and Wright*, 1997], which are sometimes observed on the same L shells as low-m FLRs [*Fenrich et al.*, 1995].
8. For large-amplitude FLRs with footpoints in regions of high ionospheric Σ_P it may be possible for the Kelvin-Helmholtz instability to be sufficiently strong to disrupt the FLR to form a vortical KH wave.

Appendix A: Kelvin-Helmholtz Stability of FLR Velocity Fields

We consider magnetic fields $\mathbf{B}_i$, densities ρ_i, and background shear velocities $\mathbf{U}_i$ in the yz plane across an infinitesimal layer at $x = 0$ ($i = 1,2$ for $x < 0$ and $x > 0$, respectively). Assuming that the waves are incompressible for simplicity, KH surface waves are governed by the equation

$$\rho_1(\omega - \mathbf{k}_{\mathrm{KH}}.\mathbf{U}_1)^2 + \rho_2(\omega - \mathbf{k}_{\mathrm{KH}}.\mathbf{U}_2)^2 = \mu_0^{-1}\left\{(\mathbf{k}_{\mathrm{KH}}.\mathbf{B}_1)^2 + (\mathbf{k}_{\mathrm{KH}}.\mathbf{B}_2)^2\right\} \tag{A1}$$

where $\mathbf{k}_{\mathrm{KH}} = (0, k_{y\mathrm{KH}}, k_{z\mathrm{KH}})$. Consequently the growth rate of the KH disturbance $\omega_{i\mathrm{KH}}$ is described by [e.g., *Cowling*, 1976]

$$\omega_{i\mathrm{KH}}^2 = \frac{\rho_1\rho_2}{(\rho_1+\rho_2)^2}\left\{\mathbf{k}_{\mathrm{KH}}.(\mathbf{U}_1 - \mathbf{U}_2)\right\}^2 - \frac{(\mathbf{k}_{\mathrm{KH}}.\mathbf{B}_1)^2 + (\mathbf{k}_{\mathrm{KH}}.\mathbf{B}_2)^2}{\mu_0(\rho_1+\rho_2)}. \tag{A2}$$

Considering instabilities occurring in the azimuthal FLR velocity shear v_{yR}, in the presence of both the Earth's background magnetic field $\mathbf{B}_0 = B_0\hat{\mathbf{z}}$ and the FLR wave magnetic field $\mathbf{b}_y = b_{yR}\hat{\mathbf{y}}$, (since b_{yR} dominates the FLR magnetic field) so that $\mathbf{B}_{1,2} = \mathbf{B}_0 \pm \mathbf{b}$, and taking $\rho_1 = \rho_2 = \rho$ and $\mathbf{U}_{1,2} = \pm v_{yR}\hat{\mathbf{y}}$ then

$$\omega_{i\mathrm{KH}}^2 = k_{y\mathrm{KH}}^2 v_{yR}^2 - k_{z\mathrm{KH}}^2 v_A^2 - k_{y\mathrm{KH}}^2 \frac{b_{yR}^2}{\mu_0 \rho}. \tag{A3}$$

Samson et al. [1996] show how the stabilizing effect of b_{yR} is negligible in comparison to the destabilizing effect of the FLR v_{yR} velocity fields for a dipole model of the Earth's magnetosphere (except very near the ionosphere), that is, $b_{yR}^2/\mu_0\rho \ll v_{yR}^2$ (especially near the equatorial antinode of b_y). Since the KH instability favors waves with $\mathbf{k.B} = 0$, we can assume $k_{z\mathrm{KH}} \ll k_{y\mathrm{KH}}$ for the fastest growing modes near the equatorial plane so that

$$\omega_{i\mathrm{KH}}^2 \approx k_{y\mathrm{KH}}^2 v_{yR}^2. \tag{A4}$$

Acknowledgments. The author thanks Gareth Chisham, Steve Schwartz and Andrew Wright for useful discussions and comments on the manuscript. The author is also very grateful to Bill Allan for many useful suggestions during the refereeing process which helped to significantly improve the paper. This work was supported by PPARC grant GR/K94133.

The Editor thanks William Allan and another referee for their assistance in evaluating this paper.

References

Allan, W., and F. B. Knox, A dipole field model for axisymmetric Alfvén waves with finite ionospheric conductivities, *Planet. Space Sci.*, *27*, 79, 1979a.

Allan, W., and F. B. Knox, The effect of finite ionospheric conductivities on axisymmetric toroidal Alfvén wave resonances, *Planet. Space Sci.*, *27*, 939, 1979b.

Allan, W., and F. B. Knox, A model of ionospheric coupling in 'toroidal-like' geomagnetic pulsations, *Tech. Rep. 698*, Phys. and Eng. Lab., Dep. of Sci. and Ind. Res., Lower Hutt, New Zealand, 1980.

Allan, W., and A. N. Wright, Large-m waves generated by small-m field line resonances via the nonlinear Kelvin-Helmholtz instability, *J. Geophys. Res.*, *102*, 19,927, 1997.

Allan, W., S. P. White, and E. M. Poulter, Magnetospheric coupling of hydromagnetic waves: Initial results, *Geophys. Res. Lett.*, *12*, 287, 1985.

Allan, W., S. P. White, and E. M. Poulter, Impulse-excited hydromagnetic cavity and field-line resonances in the magnetosphere, *Planet. Space Sci.*, *34*, 371, 1986.

Anderson, B. J., M. J. Engebretson, and L. J. Zanetti, Distortion effects in spacecraft observations of MHD toroidal standing waves: Theory and observations, *J. Geophys. Res.*, *94*, 13,425, 1989.

Barston, E. M., Electrostatic oscillations in inhomogeneous cold plasmas, *Ann. Phys.*, *29*, 282, 1964.

Borovsky, J. E., Auroral arc thicknesses predicted by various theories, *J. Geophys. Res.*, *98*, 6101, 1993.

Browning, P. K., and E. R. Priest, Kelvin-Helmholtz instability of a phase-mixed Alfvén wave, *Astron. Astrophys.*, *131*, 283, 1984.

Cally, P. S., Phase mixing and surface waves: A new interpretation, *J. Plasma Phys.*, *45*, 453, 1991.

Cally, P. S., and S. T. Maddison, A modal view of oscillations in inhomogeneous compressible MHD, *J. Plasma Phys.*, *57*, 591, 1997.

Chen, L., and A. Hasegawa, A theory of long-period magnetic pulsations, 1, Steady state excitation of field line resonance, *J. Geophys. Res.*, *79*, 1024, 1974.

Chisham, G., D. Orr, M. J. Taylor, and H. Luhr, The magnetic and optical signature of a Pg pulsation, *Planet. Space Sci.*, *38*, 1443, 1990.

Cowling, T., *Magnetohydrodynamics*. Adam Hilger, Bristol, England, 1976.

Fenrich, F. R., J. C. Samson, G. Sofko, and R. A. Greenwald, ULF high- and low-m field line resonances observed with the Super Dual Auroral Radar Network, *J. Geophys. Res.*, *100*, 21,535, 1995.

Goedbloed, J. P., Lecture notes on ideal magnetohydrodynamics, *Tech. Rep. 83-145*, Rijnhuizen, 1983.

Greenwald, R. A., and A. D. M. Walker, Energetics of long period resonant hydromagnetic waves, *Geophys. Res. Lett.*, *7*, 745, 1980.

Hasegawa, A., K. H. Tsui, and A. S. Assis, A theory of long period magnetic pulsations, 3, Local field line oscillations, *Geophys. Res. Lett.*, *10*, 765, 1983.

Hollweg, J. V., and G. Yang, Resonance absorption of compressible magnetohydrodynamic waves at thin "surfaces", *J. Geophys. Res.*, *93*, 5423, 1988.

Hughes, W. J., and D. J. L. Grard, A second harmonic geomagnetic field line resonance at the inner edge of the plasma sheet: GEOS 1, ISEE 1, and ISEE 3 observations, *J. Geophys. Res.*, *89*, 2755, 1984.

Junginger, H., and W. Baumjohann, Resonant harmonic Alfvén waves in the magnetosphere: A case study, *J. Geophys. Res.*, *89*, 10,757, 1984.

Kindel, J. M., and C. F. Kennel, Topside current instabilities, *J. Geophys. Res.*, *76*, 3055, 1971.

Kivelson, M. G., and D. J. Southwood, Resonant ULF waves: A new interpretation, *Geophys. Res. Lett.*, *12*, 49, 1985.

Kivelson, M. G., and D. J. Southwood, Coupling of global magnetospheric MHD eigenmodes to field line resonances, *J. Geophys. Res.*, *91*, 4345, 1986.

Kivelson, M. G., and D. J. Southwood, Hydromagnetic waves and the ionosphere, *Geophys. Res. Lett.*, *15*, 1271, 1988.

Kivelson, M. G., J. Etcheto, and J. G. Trotignon, Global compressional oscillations of the terrestrial magnetosphere: The evidence and a model, *J. Geophys. Res.*, *89*, 9851, 1984.

Lin, N., M. J. Engebretson, L. A. Reinleitner, J. V. Olson, D. L. Gallagher, L. J. Cahill Jr., J. A. Slavin, and A. M. Persoon, Field and thermal plasma observations of ULF pulsations during a magnetically disturbed interval, *J. Geophys. Res.*, *97*, 14,859, 1992.

Mann, I. R., A. N. Wright, and P. S. Cally, Coupling of magnetospheric cavity modes to field line resonances: A study of resonance widths, *J. Geophys. Res.*, *100*, 19,441, 1995.

Matthews, J., Hydromagnetic wave activity detected by the GOES2 double-probe experiment during 1979, *J. Geophys. Res.*, *92*, 7423, 1987.

McDiarmid, D. R., T. K. Yeoman, I. F. Grant, and W. Allan, Simultaneous observation of a traveling vortex structure in the morning sector and a field line resonance in the postnoon sector, *J. Geophys. Res.*, *99*, 8891, 1994.

Mitchell, D. G., M. J. Engebretson, D. J. Williams, C. A. Cattell, and R. Lundin, Pc5 pulsations in the outer dawn magnetosphere seen by ISEE 1 and 2, *J. Geophys. Res.*, *95*, 967, 1990.

Nielsen, E., and K. Schlegel, Coherent radar Doppler measurements and their relationship to the ionospheric electron drift velocity, *J. Geophys. Res.*, *90*, 3498, 1985.

Poulter, E. M., and W. Allan, Transient ULF pulsation decay rates observed by ground based magnetometers: The contribution of spatial integration, *Planet. Space Sci.*, *33*, 607, 1985.

Radoski, H. R., A theory of latitude dependent geomagnetic micropulsations: The asymptotic fields, *J. Geophys. Res.*, *79*, 595, 1974.

Rankin, R., B. G. Harrold, J. C. Samson, and P. Frycz, The nonlinear evolution of field line resonances in the Earth's magnetosphere, *J. Geophys. Res.*, *98*, 5839, 1993a.

Rankin, R., J. C. Samson, and P. Frycz, Simulations of driven field line resonances in the Earth's magnetosphere, *J. Geophys. Res.*, *98*, 21,341, 1993b.

Samson, J. C., J. A. Jacobs, and G. Rostoker, Latitude-dependent characteristics of long-period geomagnetic pulsations, *J. Geophys. Res.*, *76*, 3675, 1971.

Samson, J. C., T. J. Hughes, F. Creutzberg, D. D. Wallis, R. A. Greenwald, and J. M. Ruohoniemi, Observations of a detached, discrete arc in association with field line resonances, *J. Geophys. Res.*, *96*, 15,683, 1991.

Samson, J. C., B. G. Harrold, J. M. Ruohoniemi, and A. D. M. Walker, Field line resonances associated with MHD waveguides in the magnetosphere, *Geophys. Res. Lett.*, *19*, 441, 1992a.

Samson, J. C., D. D. Wallis, T. J. Hughes, F. Creutzberg, J. M. Ruohoniemi, and R. A. Greenwald, Substorm intensifications and field line resonances in the nightside magnetosphere, *J. Geophys. Res.*, *97*, 8495, 1992b.

Samson, J. C., L. L. Cogger, and Q. Pao, Observations of field line resonances, auroral arcs, and auroral vortex structures, *J. Geophys. Res.*, *101*, 17,373, 1996.

Shiokawa, K., K. Yumoto, N. Nishitani, K. Hayashi, T. Oguti, D. J. McEwan, Y. Kiyama, F. J. Rich, and T. Mukai, Quasi-periodic poleward motions of Sun-aligned auroral arcs in the high-latitude morning sector: A case study, *J. Geophys. Res.*, *101*, 19,789, 1996.

Singer, H. J., W. J. Hughes, and C. T. Russell, Standing hydromagnetic waves observed by ISEE1 and 2: Radial extent and harmonic, *J. Geophys. Res.*, *87*, 3519, 1982.

Southwood, D. J., Some features of field line resonances in the magnetosphere, *Planet. Space Sci.*, *22*, 483, 1974.

Southwood, D. J., and W. J. Hughes, Theory of hydromagnetic waves in the magnetosphere, *Space Sci. Rev.*, *35*, 301, 1983.

Streltsov, A. V., and W. Lotko, Dispersive field line resonances on auroral field lines, *J. Geophys. Res.*, *100*, 19,457, 1995.

Streltsov, A. V., and W. Lotko, The fine structure of dispersive, nonradiative field line resonance layers, *J. Geophys. Res.*, *101*, 5343, 1996.

Walker, A. D. M., Modelling of Pc5 pulsation structure in the magnetosphere, *Planet. Space Sci.*, *28*, 213, 1980.

Walker, A. D. M., The Kelvin-Helmholtz instability in the low-latitude boundary layer, *Planet. Space Sci.*, *29*, 1119, 1981.

Walker, A. D. M., R. A. Greenwald, W. F. Stewart, and C. A. Green, Stare auroral radar observations of Pc5 geomagnetic pulsations, *J. Geophys. Res.*, *84*, 3373, 1979.

Wallis, D. D., and E. E. Budzinski, Empirical models of height-integrated conductivities, *J. Geophys. Res.*, *86*, 125, 1981.

Wei, C. Q., J. C. Samson, R. Rankin, and P. Frycz, Electron inertial effects on geomagnetic field line resonances, *J. Geophys. Res.*, *99*, 11,265, 1994.

Wright, A. N., and W. Allan, Are two-fluid effects relevant to ULF pulsations?, *J. Geophys. Res.*, *101*, 24,991, 1996a.

Wright, A. N., and W. Allan, Structure, phase motion, and heating within Alfvén resonances, *J. Geophys. Res.*, *101*, 17,399, 1996b.

Wright, A. N., and M. J. Thompson, Analytical treatment of Alfvén resonances and singularities in non-uniform magnetoplasmas, *Phys. Plasmas*, *1*, 691, 1994.

Xu, B. L., J. C. Samson, W. W. Liu, F. Creutzberg, and T. J. Hughes, Observations of optical aurora modulated by resonant Alfvén waves, *J. Geophys. Res.*, *98*, 11,531, 1993.

Yeoman, T. K., D. M. Wright, T. R. Robinson, J. A. Davies, and M. Rietveld, High spatial and temporal resolution observations of an impulse-driven field line resonance in radar backscatter artificially generated with the Tromso heater, *Ann. Geophysicae*, *15*, 634, 1997.

Ian R. Mann, Department of Physics, University of Alberta, Edmonton, Alberta, Canada, T6G 2J1 (e-mail: imann@space.ualberta.ca)

(Received February 3, 1997; revised June 24, 1997; accepted August 18, 1997.)